ISSN: 2687-8402

DOI: 10.33552/OAJAA.2024.05.000616

Open Access Journal of Archaeology and Anthropology

Iris Publishers

Research Article

Tracing Impurities to Minerals: Overlapping XRF and XRD Data Sets Derived from Synchrotron Techniques

S Cipiccia[1], D Ignatiadou[2], P Bots[3], A Hamilton[3] and Effie Photos-Jones[4]*

[1]*Dept. of Medical Physics and Biomedical Engineering, University College, London, UK*

[2]*National Archaeological Museum, 10682 Athens, Greece*

[3]*Civil and Environmental Engineering, University of Strathclyde, Glasgow G1 1XQ, UK*

[4]*Analytical Services for Art and Archaeology (Ltd), Glasgow, UK and School of Humanities, University of Glasgow, Glasgow, UK*

***Corresponding author:** Effie Photos-Jones, Analytical Services for Art and Archaeology (Ltd), Glasgow, UK and School of Humanities, University of Glasgow, Glasgow, UK.

Received Date: May 01, 2023

Published Date: May 13, 2024

Abstract

Recipes for the manufacture of metals-based synthetic minerals, as well as the pharmacological preparations they formed an integral part of, are historically well documented in the Greco-Roman world. The purpose of the present research is to identify and evaluate these preparations in archaeological artifacts (labelled 'cosmetics' or 'medicines', found as pellets or mineralised powders in small ceramic/metal containers) to match 'recipe' with 'product'.

To that end, we have applied synchrotron techniques, specifically the spatial overlay of 2D XRF (major/trace elements) over XRD scans (crystalline phases), to two lead-based powders recovered from within metal vials from the 'tomb of the doctor' cemetery of Alykes, Pydna in Macedonia, Greece (4thc BCE). The aim is to ascribe major elements and impurities to spatially well-defined crystalline phases.

While the major element (i.e., Pb) clearly overlaps with the main Pb-rich phases identified (i.e., cerussite and hydrocerussite), minor/trace elements (for example Cu, Fe, Mn) equally clearly distribute themselves in a number of non-Pb based phases (i.e., quartz or amorphous). Had these elements been part of burial contamination they would likely 'blanket' cover all phases indiscriminately. Fe can be in the form of amorphous ferrihydroxides, on which Cu adsorbs; it can adhere onto quartz. When no quartz is present, organics (waxes/resins) may be the 'carriers' of these elements.

We argue that being able to differentiate between elements arising from burial environment (randomly on all phases observed) versus those integrally associated with the preparation of the powder is a powerful tool in the study of these unique samples of early pharmaceuticals technology.

Keywords: Synthetic lead carbonate (cerussite); Synchrotron techniques; 2D XRF; 2D XRD; 2D X-ray ptychography

Introduction

The method of preparation of near-pure synthetic lead carbonate *psimythion* is first reported in a recipe by Theophrastus (*On Stones*, 56) (4th c BCE) [1]. It required a block of metallic lead to be suspended over *oxos* (poor quality wine, or wine in the process of acetification) in a closed ceramic pot, over a period of ten days. During that time a white powder formed on the metal surface which was removed by scraping. Then it was ground and 'washed', leaving behind an insoluble white material, the *psimythion* of the ancient sources. This white material was collected and used as powder or shaped into pellets. As pellets, it has been recovered from ceramic pots within female graves, dated 5th -3rd c BCE. As a powder, it has

also been recovered from doctors 'medicine vials' as is the case here (see below).

The production of a lead-based white pigment continued into the Roman period (Latin *cerussa*) [2] and in the Western world, throughout the medieval period and well into the early 20th century [3]. *Psimythion* manufacture differed from later practices in that the production of the white pigment was carried out in an open vessel and with cow dung as the main source of CO_2. Indeed, this external source of CO_2 formed the basis of the famed 'Venetian ceruse' (16th century) [4]. *Psimythion* and *cerussa*/ceruse had applications as a pigment, a cosmetic or an ingredient in medicines.

We have argued [5] that the biotic component of the fermenting liquid within the closed vessel (the *oxos* or poor wine) would have been responsible for the production of sufficient CO_2 to generate cerussite on the metal surface. We suggested that the process would have initially created lead hydroxide and lead acetate, slowly converting the two to hydrocerussite in a series of reactions under first aerobic and then anaerobic conditions to largely lead carbonate. As lead hydroxide and lead acetate are water-soluble, grinding and levigating in water would have resulted in the recovery of near-pure fine and insoluble synthetic cerussite.

In this work we examine two samples of powders (rather than pellets) recovered from two metal vials, called pyxides, with tightly fitting lids (Figs. 1a, b). Pyxis Py 7821 (Figure 1a) was made of copper and contained off-white-grey sample 961, and pyxis Py 7822 (Figure 1b) of bronze (copper with c. 10% tin) containing sample 964 of similar colour. The small vials were found in the 'tomb of the doctor' (Grave 66), labelled as such on account of associated finds, at the cemetery of Alykes, Pydna in Macedonia, dating to the 4th century BCE.

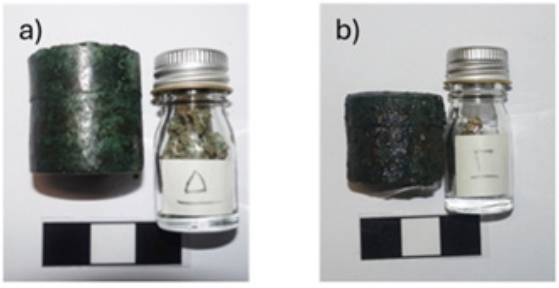

Figure 1: a) Copper pyxis Py 7821, with sample 961; Alykes, Pydna, Macedonia, Greece. b) Bronze pyxis Py 7822, with sample 964; Alykes, Pydna, Macedonia, Greece

The two samples form part of a larger collection of powders (as well as pellets) of metals-based medicinal substances currently in the process of being analysed using conventional laboratory XRD techniques [17]. In the present work we apply synchrotron techniques to establish the elemental and mineralogical compositions of only the above two.

Synchrotron Method

Synchrotron radiation has been applied successfully to the study of archaeological materials and objects of cultural heritage for several years [6-8]. The present experiment was Diamond Light Source I13-1 beamline, Harwell Science and Innovation Campus, Oxfordshire [9]. A multimodal approach was taken to understand the spatial relationship between the mineral phases present and the samples' elemental composition.

We used three different techniques: 2D X-ray fluorescence (XRF), 2D X-ray diffraction (XRD) and 2D X-ray ptychography [10]. The latter is a scanning nanoscale imaging technique, based on coherent diffraction, extremely sensitive to weak variation of electron density in the sample. Ptychography is particularly suitable for detecting slight changes within quasi-homogenous materials and for imaging very weakly absorbing samples.

2D XRF and XRD images of the samples were acquired by scanning the sample across the 20 keV X-ray beam (8μm diameter) at 5μm steps in a raster scan fashion. At each scanning position the excited fluorescence signal was recorded using a single element Vortex silicon-drift detector placed at 90 degrees off axis. The same scan was repeated to acquire the XRD data using an Excalibur detector placed just downstream from the sample to collect the diffraction patterns [11]. The scan size varied between 8x8 scans (40x40 μm^2) and 20x20 scans (100x100 μm^2). Each data collection point of the 2D scan produced a diffraction pattern and a XRF spectrum. By integrating the area under the peak corresponding to either a phase or an element's XRF emission line, 2D maps of the phase and element distributions were produced. The results are quantitative to the limit of 2D analysis. Future 3D analysis will allow for correction of the fluorescence signal, for self-absorption. No Rietveld refinement was applied to the XRD data due to the large grain size of the samples with respect to the X-ray beam size.

The 2D X-ray ptychography images were acquired by scanning the sample across the 20 keV X-ray beam (8μm diameter) at 2μm steps in a raster can fashion, using a Merlin detector, while recording the diffraction pattern in the far field. The reconstructions were based on the implementation of the ePIE algorithm [12] in PtyREX [13].

Results

The results of quantitative XRD and XRF analyses for both samples are summarised in Table 1.

Synchrotron XRD (S-XRD) analysis of 961 showed 92.4% cerussite, and 7.6% hydrocerussite while S-XRD analysis of 964 showed 78.6% cerussite, 14.3% hydrocerussite, and 7.1% quartz (Table 1). In sample 961, synchrotron XRF (S-XRF) has shown, apart from Pb, small amounts of Fe and Cu, a total of c. 7%. The quantities shown are relative rather than absolute as lighter elements, such as carbon and oxygen, which we know are present in cerussite and hydrocerussite, are not identified and quantified. In sample 964, the same two elements, Fe and Cu, make up nearly 54% of the analysed total with c. 43% Pb and c. 3% consisting of other elements (Table 1). The above compositions are considered only representative of the original sample (the totality of the powder in the vial), since homogeneity of the original sample cannot be taken for granted.

Table 1: Summary of S-XRD and S-XRF results. The relative percentage for both the XRD and XRF was calculated as relative strength of the signal for the element/phase detected.

Sample	S-XRD	S-XRF
961	92.4% cerussite, 7.6% hydrocerussite	93% Pb, 1% Fe, 6% Cu
964	78.6% cerussite, 14.3% hydrocerussite, 7.1% quartz	43.3% Pb, 26.9% Fe, 26.8% Cu, 0.38% Ca, 0.56% Ag, 0.58% Mn, 0.61% K, 0.35% Cr, 0.61% Ti

Sample 961 consists of two phases, i.e., cerussite and hydrocerussite (Figure 2b). The ptychography of sample 961 is shown in Figure 2a. XRF results indicate three elements: Pb, Cu and Fe in the relative amounts shown in Table 1 (see also XRF spectrum in Figure 2c).

Hydrocerussite reflections are only visible in the 2D analysis at d-spacing values of 4.47 Å and 4.25 Å, corresponding to angles 3.98 and 4.18 degrees respectively at 20 keV (Figure 2b). We do not detect the stronger hydrocerussite reflection, which would be visible at 2.623 Å, (equivalent to 6.78 degrees at 20 keV). Visual inspection of the raw data in the form of diffraction rings showed that while those of cerussite were complete and largely uninterrupted, the hydrocerussite rings were spotty, suggesting that the hydrocerussite crystal size was larger than, or comparable with, the beam size (6 μm), whereas the cerussite crystals were much finer. This is probable given the small sample size (40x40 μm) and data collection step size (5 μm).

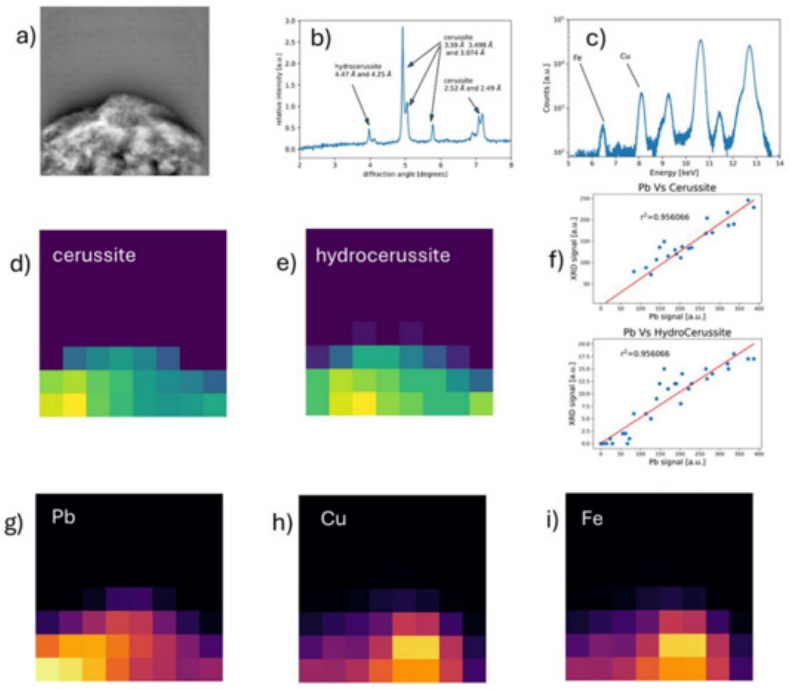

Figure 2: Sample 961 a) ptychographic image. b) XRD pattern at 20 keV showing the major peaks attributed to both cerussite and hydro cerussite. c) XRF spectrum presented in logarithmic scale to emphasize the presence of the weak peaks of Fe and Cu. d) Cerussite distribution. e) Hydrocerussite distribution. f) Pb fluorescence signal vs cerussite XRD signal and vs hydrocerussite XRD signal. g) Pb distribution. h) Cu distribution. i) Fe distribution.

The distributions of cerussite and hydrocerussite, the only two crystalline phases identified in 961, are shown in Figs. 2d and 2e respectively. As expected, there is a good linear relationship between Pb and the two Pb-carbonates (Figure 2f). In contrast, the distribution of Cu and Fe shown in Figs. 2h and 2i is distinct from that of cerussite and hydrocerussite, suggesting association with other amorphous/non-crystalline phase(s), not 'visible' in the XRD pattern.

The origin of Fe and Cu cannot be confirmed with confidence and is described as 'contamination'. Sample 'contamination' can have many sources: it could arise from the walls of the container or the burial environment at large; it could originate from the 'ore' used to make the metal (i.e., Pb); it could derive from sample preparation. In the case of 'contamination' arising from Fe/Cu present in the container/burial environment, one or both elements would likely 'blanket' cover all phases present. Figs. 2d and 2h suggest that this is not the case for sample 961. It follows that Cu and Fe are associated with a distinct but amorphous phase.

Possible candidates for the amorphous phase include: ferrihydrite, a common amorphous iron oxide occurring in soils, and on which copper can readily adsorb [14]. Ferrihydrite is also associated with iron/steel corrosion products [15]. In other words, it could have derived from the iron knife used to scrape the *psimythion* off the surface of the lead metal (as discussed earlier with reference to the Theophrastus recipe). Another amorphous phase could be organic in origin (i.e., wax/resin) with which the lead carbonate was mixed. If the latter is the case, the powder in pyxis Py 7821 would be considered a medicinal 'preparation' rather than a pure mineral ingredient.

Sample 964 consists of three phases: cerussite, hydrocerussite and quartz (Figure 3a and Table 1). The spatial separation between the Pb-rich phases (cerussite and hydrocerussite, Figs. 3f and 3g) is clear, as is that of quartz (Figure 3h). Cu and Fe are present in elevated amounts (Figure 3b) compared to the same elements in 961 but their distribution overlaps with that of quartz.

The plots of Pb vs cerussite and hydrocerussite (Figs. 3c and 3d) show a linear relationship. Pb is also well separated from Cu (Figure 3k) and Fe (Figure 3l). Sn is absent from the suite of minor elements identified (Table 1) further suggesting that contamination arising from the bronze container is less likely. In general, Sn is known to be more corrosion resistance than copper.

The Pb and Ag signal relationship is more complicated. Ag seems to distribute across the field of view. From the plot of Pb vs Ag (Figure 3e) two trends appear to emerge (or merge) as depicted by a blue and a green box (Figure 3m) corresponding to two different areas of the sample. The area outlined by the green box (Figure 3m, upper sector) not spatially associated with cerrusite, whereas the area outlined by the blue box contains cerrusite and hydrocerussite. However, considering the signal from the blue box only, Pb and Ag seem to show an exponential rather than linear dependence. This could be due to absorption of the Ag signal by Pb (note that the L-alpha line at 2.98 keV is used). Ag is clearly associated with the Pb phases and as such, with the original 'ore'. In an earlier publication we have suggested, that argentiferous lead may have been intentionally chosen for the making of *psimythion* since Ag/Pb (in grams to the ton) quantities found within *psimythion* pellets were equivalent with those found in argentiferous lead ore concentrates from Laurion, Attica, also dating to the 4th c BCE [5,16].

The Cu, Fe, Mn, Cr, K, Ti distributions (Figs. 3k, 3l, 3n, 3p, 3q, 3s) respectively show overlap with quartz, while the Ca distribution (Figure 3r) suggests the presence of another Ca-rich phase not detected by XRD. Thus, although not all phases are visible by XRD, the spatial distribution of elements in both visible and invisible phases calls for further investigation of the composition of the samples to include possible presence of organic compounds. The method constitutes a powerful tool in interrogating often made assumptions, for example that metallic minor/trace elements must reflect impurities originally present in the 'ore'.

Concluding Remarks

Using synchrotron techniques (2D XRF, 2D XRD, 2D X-ray ptychography) on two samples of ancient powders recovered from copper/bronze containers, we are able to demonstrate a clear spatial separation between mineralogically distinct phases, i.e., cerussite, hydrocerussite and quartz; also, the spatial relationship between the elements detected and the phases they belong to.

In sample 961 the 'contaminant' elements, Fe and Cu, distribute in a phase that is not visible to the XRD. The lack of spread of Cu and Fe over cerussite/hydrocerussite argues against contamination from the burial environment and/or the copper-based container and is more likely to be associated with a specific amorphous phase (organic or inorganic). Since neither element distributes over the lead-rich phases i.e., cerussite/hydrocerussite, they are unlikely to derive from the 'ore'.

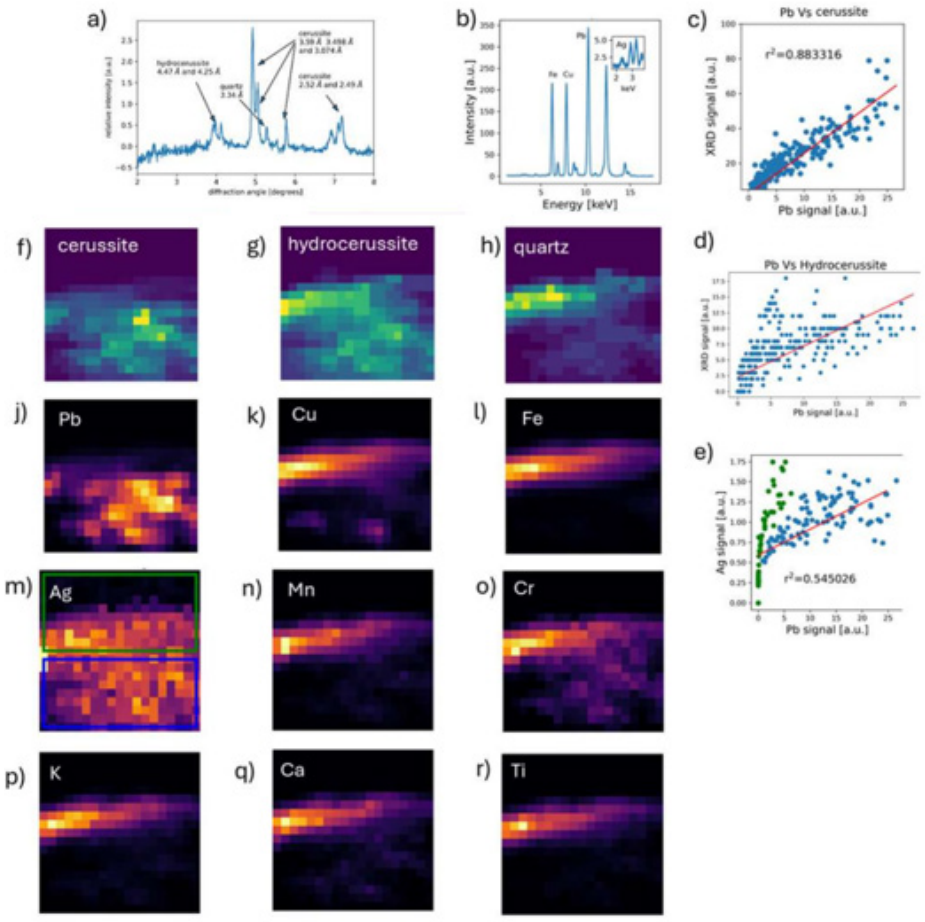

Figure 3: Sample 964. a) XRD pattern at 20 keV. b) XRF spectrum. c) Pb vs cerussite. d) Pb vs hydrocerussite. e) Pb vs Ag. f) Cerussite distribution. g) Hydrocerussite distribution. h) Quartz distribution. j-r) Spatial distribution of the identified elements, respectively Pb, Cu, Fe, Ag, Mn, Cr, K, Ca, Ti.

In sample 964, Ag does distribute over the lead-rich phases and so it can be more confidently associated with the 'ore'. On the other hand, Fe and Cu, are again located well apart from cerussite/hydrocerussite, and in this case are associated with quartz, as are Al, Ti, K, Cr, Mn. Ca belongs to a crystalline phase, also not visible by XRD and separate from the above. The presence of an organic component in either/both of the two samples needs to be investigated via organic residue analysis. We plan to examine more archaeological samples, as well as samples of experimentally prepared *psimythion* with the above method of analysis for the purpose of gaining a better insight into these intriguing materials.

Acknowledgements

This short communication contains the first results of Project MG23919 carried out at the Diamond Light Source in January 2020 (E. Photos-Jones, PI). Title: A girl's 'make-up 'or a soldier's 'first-aid'? elucidating the nature of (some) Ephorate of Antiquities of Pieria for.... in the material culture of the Greco-Roman world. The authors are grateful to the staff at the facility for their hospitality. The authors would like to thank the excavator and the Ephorate of Antiquities of Pieria for permission to sample and analyse these unique samples.

Conflict of Interest

None.

References

1. Caley E, Richards J (1956) Theophrastus *On Stones*. Ohio Univ. Press, pp. 152-156.
2. Stevenson L (1955) On the meaning of the words cerussa and psimithium (*psimythion*). Journal of the History of Medicine 10(1): 109-111.
3. Gettens RJ, Kühn H, Chase WT (1967) Lead white. Studies in Conservation 12(4): 125-139.
4. Berrie BH, Matthew LC (2011) Lead White from Venice: A Whiter Shade of Pale? In M. Spring (Ed.) Studying Old Master Paintings – Technology and Practice. London: Archetype Publications, pp. 295-301.
5. Photos-Jones E, Bots P, Oikonomou E, Hamilton A, Knapp CW (2020) On metal and 'spoiled' wine: analysing psimythion (synthetic cerussite) pellets (5th-3rd centuries BCE) and hypothesising gas-metal reactions over a fermenting liquid within a Greek pot. Archaeological and Anthropological Sciences 12(10): 243.
6. Harbottle G, Gordon BM, Jones KW (1986) Use of synchrotron radiation in archaeometry, Nuclear Instruments and Methods in Physics, Research Section B: Beam Interactions with Materials and Atoms 14(1): 116-122, ISSN 0168-583X.
7. Pantos E (2005) Synchrotron Radiation in Archaeological and Cultural Heritage Science. In: M Uda, G Demortier, I Nakai (Eds.) X-rays for Archaeology. Dordrecht, Springer.

8. Quartieri S (2015) Synchrotron Radiation in Art, Archaeology and Cultural Heritage. In: Mobilio S, Boscherini F, Meneghini C (Eds.) Synchrotron Radiation. Berlin, Heidelberg, Springer.

9. Cipiccia S, Batey D, Shi X, Williams S, Wanelik K, et al. (2019) Multi-scale multi-dimensional imaging at I13-coherence branchline in Diamond light source. AIP Conference Proceedings 15, 2054 (1): 050005.

10. Rodenburg JM, Hurst AC, Cullis AG, Dobson BR, Pfeiffer F, et al. (2007) Hard-x-ray lensless imaging of extended objects. Physical Review Letters 98.

11. Tartoni N et al. (2012) Excalibur: A three million pixels photon counting area detector for coherent diffraction imaging based on the Medipix3 ASIC, Proc. IEEE Nucl. Sci. Symp. Med. Imag. Conf. Record (NSS/MIC).

12. Maiden AM, Rodenburg JM (2009) An improved ptychographical phase retrieval algorithm for diffractive imaging. Ultramicroscopy, 109(10):1256-1262.

13. Batey D (2014) Ptychographic Imaging of Mixed States. Unpublished PhD thesis, University of Sheffield.

14. Seda N, Koenigsmark NF, Vadas TM (2016) Sorption and coprecipitation of copper to ferrihydrite and humic acid organomineral complexes and controls on copper availability. Chemosphere 147: 272-278.

15. Cudennec Y, Lecerf A (2006) The transformation of ferrihydrite into goethite or hematite, revisited. Journal of Solid-State Chemistry 179(3): 716-722.

16. Photos-Jones E (2023) Beyond the silver 'owls': Laurion lead and its contribution to synthetic lead-based minerals for the health care/ medicines market (4th century BC). In: F Hulek, H Lohmann, S Nomicos, A Hauptmann (Eds.) Laurion Interdisciplinary Approaches to an Ancient Greek Mining Landscape Including Selected Papers Presented at the International Conference 'Ari and the Laurion from Prehistoric to Modern Times' (Bochum 2019) Der Anschnitt 50: 245-252.

17. Ignatiadou D, Bots P, Ribbechini DE, Katsifas Ch, Photos-Jones E (forthcoming) The tomb of the doctor: a study of Hippocratic mineral 'therapeutics' (4th c BCE).